

Molecular Dynamics Simulations Elucidate the Synergy of C₆₀ and Low-Energy Ar Cobombardment for Molecular Depth Profiling

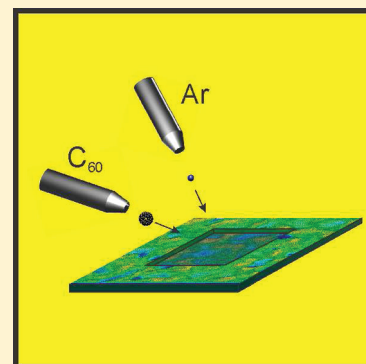
Zachary J. Schiffer,[†] Paul E. Kennedy,[†] Zbigniew Postawa,[‡] and Barbara J. Garrison^{*,†}

[†]Department of Chemistry, 104 Chemistry Building, Penn State University, University Park, Pennsylvania 16802, United States

[‡]Smoluchowski Institute of Physics, Jagiellonian University, ul. Reymonta 4, 30-059 Kraków, Poland

ABSTRACT: The use of cluster beams in secondary ion mass spectrometry enables molecular depth profiling, a technique that is essential to many fields. The success of the technique often hinges upon the chemical nature of the substrate, the kinetic energy and incident angle of the primary cluster ion beam, and the sample temperature. It has been shown experimentally that the quality of depth profiles can be improved with cobombardment by a C₆₀ cluster beam and a low-energy argon (Ar) beam. We present molecular dynamics simulations to elucidate the mechanistic reasons for the improved molecular depth profiles with an aim of understanding whether this cobombardment approach is generally applicable. We conclude that the low-energy Ar beam breaks up the surface topology created by the C₆₀ beam, increasing the sputtering yield and reducing the buildup of chemical damage. The simulations also suggest that an equivalent result could be achieved without the Ar cobombardment by optimizing the conditions of the C₆₀ beam.

SECTION: Surfaces, Interfaces, Catalysis



The introduction of cluster ion beams in the analytical technique of secondary ion mass spectrometry (SIMS) has opened the door to a new world of 3D *molecular* depth profiling of numerous materials, a measurement unattainable with any other technique.¹ Although there are many successful examples of molecular depth profiling with cluster beams, especially with C₆₀ bombardment, there are also examples for which the molecular depth profile is not successful.² For molecular depth profiling, success is defined as measuring a constant signal of the molecular species in all depth regions where the molecule was originally present. Depending on the system, lack of success can be due to nonoptimal experimental conditions or unfortunate chemistry of the system, including poor ion yields.² Experimental conditions that tend to improve the quality of molecular depth profiles include higher beam energies, more grazing polar angles of incidence, sample cooling, and sample rotation.³ Molecular solids that have high sputtering yields and polymers such as poly(methyl methacrylate) and poly(lactic acid) that readily form gaseous products tend to depth profile well, whereas polymers that readily cross-link such as polyethylene and polystyrene do not tend to depth profile well.² The factors that control ion yields largely remain a mystery, although the use of C₆₀ projectiles can enhance the ion fraction.⁴

General experimental strategies that improve depth profiles such as using a grazing angle of incidence or applying sample cooling are straightforward to implement. It is more of a challenge to find a strategy to fix unfortunate chemistry in molecular solids. An intriguing set of experiments from Shyue and coworkers shows promise of assisting depth profiles by cobombardment of the system with C₆₀ and low-energy Ar ions.^{5–13} This strategy for eroding samples has, as yet, been

implemented by only one research group because most SIMS instruments with C₆₀ ion beams do not also have a low-energy Ar ion beam. We have performed molecular dynamics (MD) computer simulations that provide insight into the interplay of effects in the solid by C₆₀ cobombardment with low-energy Ar ions. Our conclusion is that C₆₀ bombardment creates an anisotropic roughened surface that the Ar bombardment ameliorates. It is essential that the energy of the Ar beam remains below 200 eV so that no damage is induced beyond the altered layer created by the C₆₀ beam. In addition, the simulations reveal that the experimental C₆₀ conditions are not optimal for the best quality depth profiles and suggest that changing the C₆₀ beam conditions would be an alternative experimental solution for experimentalists with similar instruments than the addition of low energy Ar bombardment.

The experiments involve surface analysis by X-ray photoelectron spectroscopy (XPS) after erosion by C₆₀ and Ar bombardment, although for some organic polymeric systems, SIMS measurements have been performed as well.^{5,6} The C₆₀ source operates at 10 keV at a 70° polar angle of incidence, and the Ar source operates from 100 to 400 eV of incident energy at a 45° polar angle of incidence oriented 33° from the C₆₀ beam. The ion current emitted by the Ar source is 30 times larger than the ion beam current produced by the C₆₀ gun. The experiments show that improvement of the depth profile requires the Ar energy to be 200 eV or less; otherwise, the composition of the substrate changes, as measured by XPS.⁶ Measurements have been made of

Received: September 5, 2011

Accepted: October 2, 2011

Published: October 03, 2011

Table 1. Total Sputtering Yield, Y_{tot} , in Units of Molecular Equivalents of Benzene, Sputtered Volume, V_s , the Average Number of Damaged Molecules That Remain in the Bombarded Solid, N_D , and the Ratio of Sputtered to Damaged Molecules, Y_{tot}/N_D , for Ar and C_{60} Projectiles Bombarding a Crystal of Solid Benzene

projectile	Y_{tot}	V_s (nm ³)	N_D	Y_{tot}/N_D
100 eV Ar	4.9 ± 0.3	0.6 ± 0.03	0.8 ± 0.2	6.1 ± 0.4
200 eV Ar	6.9 ± 0.6	0.8 ± 0.08	3.2 ± 0.3	2.2 ± 0.2
300 eV Ar	9.1 ± 0.9	1.1 ± 0.1	5.0 ± 0.4	1.8 ± 0.2
400 eV Ar	11.5 ± 1.4	1.4 ± 0.2	6.9 ± 0.4	1.7 ± 0.2
10 keV C_{60} 0°	745	90	14	53
10 keV C_{60} 70°	342	41	9	38
15 keV C_{60} 0°	1242 ± 28	150 ± 3	88 ± 3	14.2 ± 0.6

the sputtering yields without and with Ar cobombardment for the Ar energy of 200 eV. For the polymer poly(ethylene terephthalate), the cosputtering removes the high mass species from the mass spectrum, but the abundance of low mass species is enhanced. This observation indicates that the atomic projectile breaks organic molecules. The sputter rates are 1.58 nm³ per incident ion for C_{60} bombardment by itself and 1.94 nm³ per incident C_{60} ion with cobombardment by Ar. For poly(methyl methacrylate), the sputter rates are 2.52 nm³ per incident ion for only C_{60} bombardment and 2.97 nm³ per incident C_{60} ion with cobombardment by Ar. The latest study also shows that cobombardment produces smoother surfaces than bombardment by C_{60} alone.⁵ Low-energy inert gas bombardment does not produce a quality depth profile, nor does it eject large species.^{5,14} Bombardment with low-energy Cs⁺, however, has produced molecular depth profiles,¹⁴ but the mechanism for this process is connected with improving the ion yield due to the low ionization energy of Cs. The most intriguing question that results from the Shyue and coworker studies is the nature of the synergistic effects in the solid due to the cosputtering configuration.

Molecular dynamics modeling has already been utilized successfully to understand many aspects of projectile–surface interactions relevant to SIMS.¹⁵ The goal of the current study is to discern how the low-energy Ar bombardment might assist the C_{60} bombardment process for depth profiling, when neither the C_{60} nor the Ar bombardment by itself is effective. The key must lie in the applied energy range, as determined from experiment; that is, the Ar bombardment must be at 200 eV or less. Solid benzene has been chosen as a computational model because we have utilized this system successfully in previous studies.¹⁵

There are several possible reasons that may account for better depth profiling in cosputtering experiments. First, as predicted by an erosion dynamics model, the total sputtering yield relative to the damage created should be large for effective depth profiling.¹⁶ The experimental sputtering yield⁵ reported by You et al. ranges from 1 to 3 nm³ per incident ion. This yield is, however, very small compared with, for example, the experimental yield for 40 keV C_{60} bombardment of cholesterol at 73° incident angle for which the yield is two orders of magnitude larger.¹⁷ The total sputtering yield⁵ reported by You et al. is 20–30% larger if the auxiliary Ar beam is present. Based on the MD simulations, the total sputtering yields from solid benzene in both molecular equivalents and sputtered volume for 100–400 eV Ar bombardment at 45° incident polar angle, 10 keV C_{60} bombardment at 0° and 70° incident polar angle and 15 keV C_{60} bombardment at

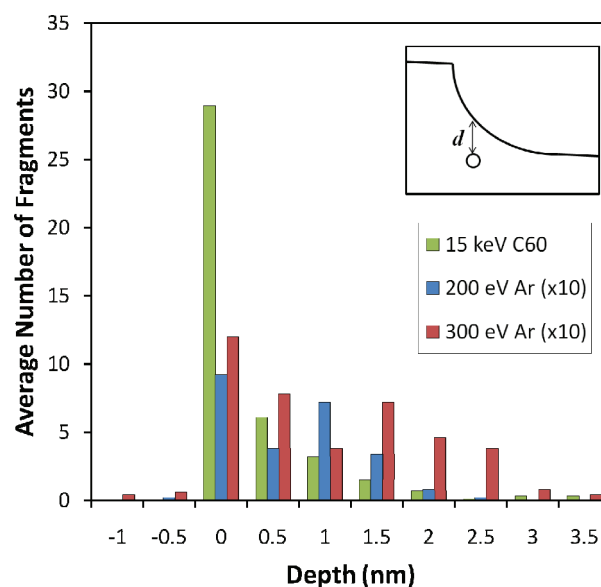


Figure 1. Depth dependence of the average number of fragments created by 15 keV C_{60} at normal incidence and by 200 and 300 eV Ar at 45° impact angle. The depth, d , is measured as the distance from the walls of the final crater for the 15 keV C_{60} trajectory, as shown in the inset, and from the top of the initial surface for the Ar trajectories.

0° are given in Table 1. Although the calculated yields for this low binding energy solid are larger than the experimental values, the yield for Ar bombardment is more than an order of magnitude lower than the calculated sputtering yield for 10–15 keV C_{60} bombardment. This observation eliminates the hypothesis that the Ar beam is increasing the sputtering yield to the point observed in experiment.

Another important observation from the experiment is that the measured ion signal is decreasing rapidly with the initial projectile fluence.⁵ Such behavior is typical for depth profiling of many polymers and indicates that the chemical composition of the near surface region of the organic sample is substantially modified. Computer simulations show that the most efficient channel of particle emission is hydrogen removal.¹⁸ Such a process will ultimately lead to dehydrogenation of the near surface volume and stimulate the formation of a network of cross-linked molecules, a carbonized overlayer, or both. Both of these processes will lead to drastic reduction of the sputtering yield, which is indeed observed.^{2,18}

The Ar beam could break up the damage left by the C_{60} beam, as proposed by the experimental researchers.⁵ The key point in this hypothesis is that the additional damage induced by the auxiliary beam cannot extend beyond the damage induced by the primary beam. Shown in Figure 1 is the damage left in the sample as a function of depth for different bombardment conditions. The damage for the C_{60} bombardment is defined as the average number of fragments located at a given depth measured as the distance from the walls of the final crater, as shown in the inset to Figure 1. The choice of 200 and 300 eV for Ar bombardment is based on the experimental observation that the best improvement for Ar cobombardment is for incident energies below 200 eV. Most of the damage induced by the 200 eV Ar bombardment is confined to the top 2 nm of the sample, whereas the 300 eV Ar does damage to depths greater than 3 nm. The amount of damage with the 10 keV C_{60} bombardment at 70° polar angle

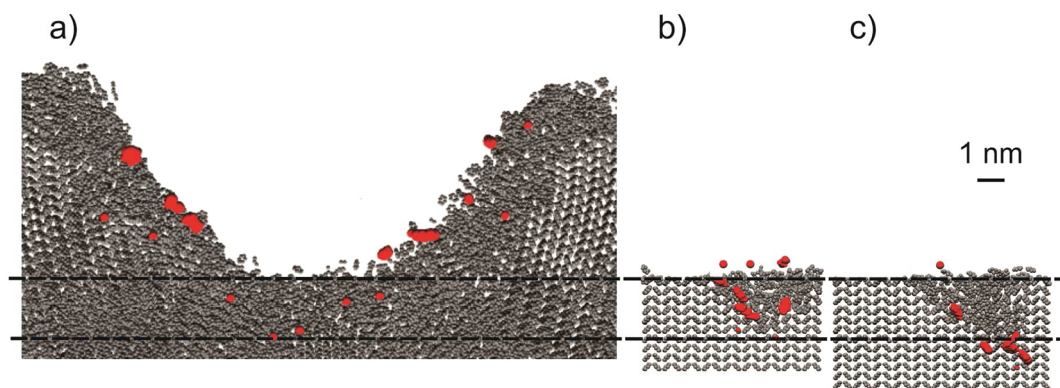


Figure 2. Location of the molecular fragments (red and enlarged) created by (a) 15 keV C_{60} bombardment of solid benzene at a normal incidence and (b) 200 and (c) 300 eV Ar at 45° impact angle. The trajectories are selected to represent average damage. Only the molecules located in a slice 5 nm wide, centered at the point of projectile impact, are shown. In addition, for nondamaged molecules, only the C atoms are shown. The snapshots are aligned so that the surfaces of the Ar bombarded samples correspond to the bottom of the crater induced by C_{60} impact to easily compare the damage induced by these two projectiles. The scale bar refers to all images.

of incidence is very low. This simulation was performed with a large crystal using a computationally intensive interaction potential. Consequently, we do not have a significant enough number of trajectories calculated for this impact angle to determine reliable damage statistics for comparison. Therefore, as an upper estimate of the damage, we analyze the damage created by 15 keV C_{60} bombardment at normal incidence. (unpublished results) It is clear that the depth of the damage created by the 200 eV Ar bombardment is a better match than the 300 eV bombardment to the C_{60} bombardment.

A graphical depiction of this information is presented schematically in Figure 2, where a 5 nm slice of the crater region for C_{60} bombardment is shown. The red molecules are damaged molecules. Also shown is damage associated with trajectories that exhibit an average number of damaged molecules for 200 and 300 eV Ar bombardment. Clearly, the 200 eV Ar bombardment confines its damage to the altered layer of the C_{60} bombardment, whereas the 300 eV Ar bombardment extends the damage into pristine sample.

Finally, there is another possibility that may contribute to the enhancement of the depth profiles^{5,6} of organic solids with cobombardment by C_{60} and 200 eV Ar when compared with C_{60} bombardment. High-fluence simulations of C_{60} impacts show that C_{60} bombardment at 70° incidence creates a roughened surface with elongated ridges and valleys parallel to the beam direction, as shown in depth profiling calculations on Ag.¹⁹ These simulations show, however, that by using sample rotation, these elongated ridges and valleys do not form, the surface gets smoother, and the sputtering yield increases by $\sim 10\%$. This value is actually comparable to the yield increase reported by You et al. for organic, polymeric samples.⁵ Indeed, with cobombardment, the reported experimental yield increases by 18–23%, and the surface roughness decreases.⁵ Therefore, we propose that the Ar beam, which is oriented 33° with respect to the C_{60} beam, is breaking up the ridges formed by the C_{60} bombardment, effectively smoothing the surface. As already mentioned, because of a very low (<200 eV) kinetic energy of the incident Ar projectiles, the damage induced by these projectiles is kept in the same region as damage created by the C_{60} bombardment. A smooth surface would increase the yield slightly, thus increasing the depth profiling ability.¹⁹ Taking into account this explanation for the enhancement due to cobombardment by the cluster and atomic projectiles, we would not expect this synergy to exist for

angles of incidence closer to the surface normal, nor would we expect the enhancement for beam conditions that give much higher yields. For example, in Table 1, the sputtering yield for C_{60} bombardment at normal incidence is twice as large as that at 70° , and increasing the kinetic energy increases the yield even further. A change in the C_{60} conditions might be just as effective in improving the depth profile as cobombardment with low-energy Ar ions.

The cobombardment approach has been implemented for inorganic materials^{7–13} in addition to the organic materials considered here. Undoubtedly, the low-energy Ar bombardment is also smoothing those surfaces. In addition, as proposed by the experimental investigators, the Ar bombardment is assisting in the removal of carbon residue left by the C_{60} beam.

In summary, MD simulations are utilized to elucidate the reasons for improved depth profiling capabilities when a C_{60} beam with 10 keV incident energy at a polar angle of 70° cobombards a molecular solid along with low-energy Ar projectiles. The simulations show that the sputtering enhancement observed in the cospattering experiment cannot be attributed to material removal by the additional ion beam. Instead, the observed increase can be attributed to reduction of the surface morphology. High-fluence simulations indicate that the grazing angle of incidence of the C_{60} beam creates anisotropic topology in the surface. The Ar bombardment breaks up the topology, creating a smoother surface and thus a higher yield. The key point is, however, to keep the damage induced by the auxiliary beam in the same region as the damage by the C_{60} cluster bombardment. This can be accomplished by maintaining the Ar incident energy to <200 eV. Ultimately, the simulations indicate that the enhancement by the Ar cobombardment should be most effective for the specific C_{60} beam conditions utilized by the experimentalists and does not show the potential for a generic fix of unfortunate chemistry in molecular depth profiling.

COMPUTATIONAL DETAILS

MD simulations¹⁵ are used to model the effect of energetic particle bombardment on an organic substrate. The choice of system is a balance between a realistic description of the experimental system and a computationally practical one. Moreover, it is our assumption that the effect of the Ar and C_{60} cobombardment is generic to hydrocarbon species, and thus we

choose to use our prototypical hydrocarbon system of benzene. The description of the interaction energies and forces among the atoms is based on the AIREBO potential,²⁰ which combines long-ranged interactions with the short-ranged Brenner REBO potential.^{21,22} The Moliere potential,²³ a basic potential for high-energy collisions, is used to describe the argon interactions with the carbon and hydrogen atoms.

To understand the relationship between Ar and C₆₀, simulations of both Ar and C₆₀ bombardment were performed. Argon atoms with 100, 200, 300, and 400 eV incidence energies were used to bombard benzene solids at an incident polar angle of 45°. Fifty trajectories were run at each incident energy. To describe all of the action in the solid, two different sizes of benzene solids were chosen, the first for 100 and 200 eV argon bombardment and the second for 300 and 400 eV argon bombardment. The first solid was a rectangular prism²⁴ measuring approximately 6.56 nm × 5.64 nm in width by 3.45 nm in depth and consisting of 1080 benzene molecules. The second solid was a rectangular prism measuring approximately 8.03 nm × 6.59 nm × 4.15 nm and consisting of 1848 benzene molecules. Periodic boundary conditions were used in the horizontal directions. A rigid layer of 0.347 nm covers the bottom of the solid with a stochastic layer of 0.736 nm immediately above it. For the 10 keV C₆₀ bombardment, a hemisphere solid of benzene with a radius of 21.2 nm was used. A rigid layer of 0.7 nm surrounds the solid with a stochastic layer of 3.3 nm immediately inside it. There are 175 434 benzene molecules in the hemisphere. Because the simulation of such a large system using a sophisticated many-body hydrocarbon potential is computationally very expensive, only one trajectory was run for cases where a qualitative comparison was needed. Such an approach has been shown to be justifiable for cluster bombardment.¹⁵ However, as more trajectories should be sampled when making quantitative predictions, we have used the data for 10 trajectories of 15 keV C₆₀ impact at normal incidence using a blended scheme. In this scheme, the AIREBO potential is utilized in regions where reactions occur, and a coarse-grained representation is used in regions where the molecules remain intact (unpublished results).

AUTHOR INFORMATION

Corresponding Author

*Phone: 814-863-2103. Fax: 814-865-5143. E-mail: bjg@psu.edu.

ACKNOWLEDGMENT

We gratefully acknowledge financial support from the National Science Foundation grant no. CHE-0910564 and the Polish Ministry of Science and Higher Education Program no. PB1839/B/H03/2011/40. Computational resources were provided by the Research Computing and Cyberinfrastructure group at Penn State University.

REFERENCES

- (1) Wucher, A.; Winograd, N. Molecular Sputter Depth Profiling Using Carbon Cluster Beams. *Anal. Bioanal. Chem.* **2010**, *396*, 105–114.
- (2) Mahoney, C. M. Cluster Secondary Ion Mass Spectrometry of Polymers and Related Materials. *Mass Spectrom. Rev.* **2010**, *29*, 247–293.
- (3) Zheng, L. L.; Wucher, A.; Winograd, N. Depth Resolution During C₆₀⁺ Profiling of Multilayer Molecular Films. *Anal. Chem.* **2008**, *80*, 7363–7371.
- (4) Weibel, D.; Wong, S.; Lockyer, N.; Blenkinsopp, P.; Hill, R.; Vickerman, J. C. A C₆₀ Primary Ion Beam System for Time of Flight Secondary Ion Mass Spectrometry: Its Development and Secondary Ion Yield Characteristics. *Anal. Chem.* **2003**, *75*, 1754–1764.
- (5) You, Y. W.; Chang, H. Y.; Lin, W. C.; Lee, S. H.; Kao, W. L.; Yen, G. J.; Chang, C. J.; Liu, C. P.; Huang, C. C.; Liao, H. Y.; et al. Molecular Dynamic-Secondary Ion Mass Spectrometry (D-Sims) Ionized by Co-Sputtering with C₆₀⁺ and Ar⁺. *Rapid Commun. Mass Spectrom.* **2011**, *25*, 2897–2904.
- (6) Yu, B. Y.; Chen, Y. Y.; Wang, W. B.; Hsu, M. F.; Tsai, S. P.; Lin, W. C.; Lin, Y. C.; Jou, J. H.; Chu, C. W.; Shyue, J. J. Depth Profiling of Organic Films with X-Ray Photoelectron Spectroscopy Using C₆₀⁺ and Ar⁺ Co-Sputtering. *Anal. Chem.* **2008**, *80*, 3412–3415.
- (7) Lin, W. C.; Lin, Y. C.; Wang, W. B.; Yu, B. Y.; Iida, S.; Tozu, M.; Hsu, M. F.; Jou, J. H.; Shyue, J. J. Effect of Fabrication Process on the Microstructure and the Efficiency of Organic Light-Emitting Diode. *Org. Electron.* **2009**, *10*, 459–464.
- (8) Lin, W. C.; Liu, C. P.; Kuo, C. H.; Chang, H. Y.; Chang, C. J.; Hsieh, T. H.; Lee, S. H.; You, Y. W.; Kao, W. L.; Yen, G. J.; et al. The Role of the Auxiliary Atomic Ion Beam in C₆₀⁺-Ar⁺ Co-Sputtering. *Analyst* **2011**, *136*, 941–946.
- (9) Lin, W. C.; Wang, W. B.; Lin, Y. C.; Yu, B. Y.; Chen, Y. Y.; Hsu, M. F.; Jou, J. H.; Shyue, J. J. Migration of Small Molecules During the Degradation of Organic Light-Emitting Diodes. *Org. Electron.* **2009**, *10*, 581–586.
- (10) Lin, Y. C.; Chen, Y. Y.; Yu, B. Y.; Lin, W. C.; Kuo, C. H.; Shyue, J. J. Sputter-Induced Chemical Transformation in Oxoanions by Combination of C₆₀⁺ and Ar⁺ Ion Beams Analyzed with X-Ray Photoelectron Spectrometry. *Analyst* **2009**, *134*, 945–951.
- (11) Yu, B. Y.; Lin, W. C.; Chen, Y. Y.; Lin, Y. C.; Wong, K. T.; Shyue, J. J. Sputter Damage in Si (001) Surface by Combination of C₆₀⁺ and Ar⁺ Ion Beams. *Appl. Surf. Sci.* **2008**, *255*, 2490–2493.
- (12) Yu, B. Y.; Lin, W. C.; Huang, J. H.; Chu, C. W.; Lin, Y. C.; Kuo, C. H.; Lee, S. H.; Wong, K. T.; Ho, K. C.; Shyue, J. J. Three-Dimensional Nanoscale Imaging of Polymer Bulk-Heterojunction by Scanning Electrical Potential Microscopy and C₆₀⁺ Cluster Ion Slicing. *Anal. Chem.* **2009**, *81*, 8936–8941.
- (13) Yu, B. Y.; Liu, C. Y.; Lin, W. C.; Wang, W. B.; Lai, I. M.; Chen, S. Z.; Lee, S. H.; Kuo, C. H.; Kao, W. L.; You, Y. W.; et al. Effect of Fabrication Parameters on Three-Dimensional Nanostructures and Device Efficiency of Polymer Light-Emitting Diodes. *ACS Nano* **2010**, *4*, 2547–2554.
- (14) Wehbe, N.; Houssiau, L. Comparative Study of the Usefulness of Low Energy Cs⁺, Xe⁺, and O₂⁺ Ions for Depth Profiling Amino-Acid and Sugar Films. *Anal. Chem.* **2010**, *82*, 10052–10059.
- (15) Garrison, B. J.; Postawa, Z. Computational View of Surface Based Organic Mass Spectrometry. *Mass Spectrom. Rev.* **2008**, *27*, 289–315.
- (16) Cheng, J.; Wucher, A.; Winograd, N. Molecular Depth Profiling with Cluster Ion Beams. *J. Phys. Chem. B* **2006**, *110*, 8329–8336.
- (17) Kozole, J.; Wucher, A.; Winograd, N. Energy Deposition During Molecular Depth Profiling Experiments with Cluster Ion Beams. *Anal. Chem.* **2008**, *80*, 5293–5301.
- (18) Végh, J. J.; Graves, D. B. Molecular Dynamics Simulations of Ar⁺–Organic Polymer Interactions. *Plasma Processes Polym.* **2009**, *6*, 320–334.
- (19) Garrison, B. J.; Postawa, Z. Effect of Sample Rotation on Surface Roughness with keV C₆₀ Bombardment in Secondary Ion Mass Spectrometry (Sims) Experiments. *Chem. Phys. Lett.* **2011**, *506*, 129–134.
- (20) Stuart, S. J.; Tutein, A. B.; Harrison, J. A. A Reactive Potential for Hydrocarbons with Intermolecular Interactions. *J. Chem. Phys.* **2000**, *112*, 6472–6486.
- (21) Brenner, D. W.; Shenderova, O. A.; Harrison, J. A.; Stuart, S. J.; Ni, B.; Sinnott, S. B. A Second-Generation Reactive Empirical Bond Order (Rebo) Potential Energy Expression for Hydrocarbons. *J. Phys.: Condens. Matter* **2002**, *14*, 783–802.
- (22) Brenner, D. W. Empirical Potential for Hydrocarbons for Use in Simulating the Chemical Vapor-Deposition of Diamond Films. *Phys. Rev. B* **1990**, *42*, 9458–9471.
- (23) Torrens, I. M. *Interatomic Potentials*; Academic Press: New York, 1972.
- (24) Cox, E. G. Crystal Structure of Benzene. *Rev. Mod. Phys.* **1958**, *30*, 159.